Computational Materials Science 50 (2010) 690–697

Contents lists available at ScienceDirect

Computational Materials Science

journal homepage: www.elsevier.com/locate/commatsci

Simulation of dynamic recrystallization in solder interconnections during thermal cycling

J. Li *, H. Xu, T.T. Mattila, J.K. Kivilahti, T. Laurila, M. Paulasto-Kröckel

Department of Electronics, Aalto University School of Science and Technology, 02150, Finland

ARTICLE INFO

Article history:
Received 31 August 2010
Received in revised form 17 September 2010
Accepted 27 September 2010
Available online 23 October 2010

Keywords:
Dynamic recrystallization
Finite element method
Lead-free solder
Monte Carlo method
Reliability

ABSTRACT

In the present study, an algorithm, combining the Potts model based Monte Carlo (MC) and finite element methods, is developed in order to predict the dynamic recrystallization of tin in tin-rich lead-free solder interconnections during thermal cycling. A correlation between real time and MC simulation time is established. The phenomenon that intermetallic particles provide favorable sites for nucleation of new tin grains in solder matrix is also simulated. It is demonstrated that the present algorithm predicts the incubation period of the recrystallization as well as the growth tendency of the recrystallized regions, in a way consistent with the experimental findings. This quantitative description of the microstructural changes will contribute significantly to the reliability studies of solder interconnections.

1. Introduction

Solder alloys are widely used bonding materials in electronics industry. The reliability concerns for solder interconnections, which provide both mechanical and electronic connections, are rising with the increasing use of highly integrated components in portable electronic products. In service, almost all products are subjected to thermal cycles as a result of temperature changes due to component internal heat dissipation or ambient temperature changes. The existence of coefficient of thermal expansion (CTE) mismatches between dissimilar materials results in thermo-mechanical fatigue of the solder interconnections which leads to the cracking of the interconnections and failures of the electronic devices. Although numerous results of accelerated thermal cycling tests have been published in the literatures, only a few investigations paid attention to the microstructural changes, especially recrystallization, in the bulk solder [1–5].

A thorough understanding of the recrystallization phenomenon in solder interconnections is of great importance to the reliability studies of electronic products. The as-solidified microstructure of solder interconnections are usually composed of several large tin-based colonies separated by high angle boundaries [1,5]. Experimental observations indicate that the microstructure of solder may change significantly during the operation of products. The as-solidified microstructure can transform locally into a more or less equiaxed grain structure by recrystallization [1–5]. In the recrystallized region a continuous network of high angle grain boundaries provides favorable sites for cracks to nucleate and to propagate intergranularly, which can lead to an early failure of the component.

For decades, the industry has used recrystallization to control microstructures, and static recrystallization of structural metals after deformation is probably the best understood recrystallization process [6]. On the other hand, dynamic recrystallization during cyclic deformation, which occurs in solder interconnections, has received much less attention and is still poorly understood. This is because the related microstructural events are highly complex from the microstructural point of view. The major understanding of this subject is briefly summarized as follows. During cyclic thermomechanical loading, a fraction of the energy associated with the plastic deformation of solder interconnections is stored in the metal, mainly in the form of dislocations. The stored energy is subsequently released during restoration, which can be divided into three main processes: recovery, primary recrystallization and grain growth. Recovery and recrystallization are two competing processes, which are driven by the increased internal energy of the deformed solder. Recovery decreases the driving force for recrystallization and thus hinders the initiation of recrystallization. In high stacking fault energy metals such as Sn, the release of stored energy takes place so effectively by recovery that recrystallization will not practically take place [6–8]. Studies have shown that after a single deformation static recrystallization rarely occurs in Sn-rich solders [8]. However, under

* Corresponding author. Tel.: +358 445559692.
E-mail addresses: juliusjueli@gmail.com, jueli@cc.hut.fi (J. Li).

0927-0256/$ - see front matter © 2010 Elsevier B.V. All rights reserved.
doi:10.1016/j.commatsci.2010.09.035

dynamic loading conditions such as in thermal cycling tests, recrystallization often occurs in the high stress concentration regions of solder interconnections [1,3,5,8]. In addition to the aforementioned experimental observations, there is a strong need for quantitative models which can explicitly predict microstructural changes in solders during thermal cycling in order to establish a physically meaningful lifetime estimate. The motivation for the present simulation work is to offer a better understanding and to provide a quantitative description of the restoration processes in solder interconnections.

Various models have been developed to simulate microstructural evolution, such as vertex model, Monte Carlo (MC) Potts model, phase field model, and cellular automata (CA) model [6,9]. For modeling recrystallization, the MC Potts model and CA model are perhaps the two most popular candidates [7,9,10]. In general, the MC Potts model and CA model are similar to each other since both models include a lattice, use discrete orientations and describe stored energy in terms of a scalar stored energy term [6,9]. The MC Potts model provides a convenient way to simulate the changes in microstructures and it has been successfully applied to simulate the recrystallization process in solder interconnections [11] as well as in many other applications, e.g. [12–14]; thereby, it is also employed in the current algorithm.

In the present approach, the finite element method is utilized to model macroscale inhomogeneous deformation, and the MC Potts model is utilized to model the mesoscale microstructural evolution. Similar hybrid models, combining FEM and recrystallization models, have been proposed in earlier work. For instance, Zambaldi et al. [15] modeled the indentation deformation and recrystallization of a single crystal nickel-based superalloy, and Raabe and Becker [16] combined a plasticity finite element model with a probabilistic cellular automaton for simulating primary static recrystallization of aluminum.

In the current work, the influence of the activation energy on time scaling is discussed. Compared to the in situ experimental observations, a correlation between real time and MC simulation time is established. The energy minimization principle is utilized to simulate the process of primary recrystallization while the total energy of the system consists of the grain boundary energy and the volume stored energy. In addition, for the first time, the effects of intermetallic particles (Cu_6Sn_5 and Ag_3Sn) on recrystallization in solder matrix are included in the simulation.

The paper is organized as follows. Section 2 reports the model set up and the details of the simulation process, Section 3 presents simulation results as well as experimental verifications, and Section 4 contains the conclusions drawn from the model structure, the simulation process, and the results.

2. Model set up and simulation process

Thermal cycling (TC) tests are accelerated fatigue tests, which subject the components and solder interconnects to alternating high and low temperature extremes [17]. The tests are conducted to determine the ability of the parts to resist a specified number of temperature cycles from a specified high temperature to a specified low temperature with a certain ramp rate and dwell time. A typical temperature profile for a TC test is shown in Fig. 1.

Each thermal cycle can be regarded as 'deformation + annealing' and TC tests normally last several thousand cycles before failures of the components are detected. The algorithm developed in this work is based on the principle that the stored energy of solder is gradually increased during each thermal cycle. Even though recovery consumes a certain amount of the energy, the net change of the energy is always assumed to be positive due to the fact that newly recrystallized grains appear after a certain number of thermal cycles. When a critical value of the energy is reached, recrystallization is initiated. The stored energy is released through the nucleation and growth of new grains, which gradually consume the strain-hardened matrix of high dislocation density.

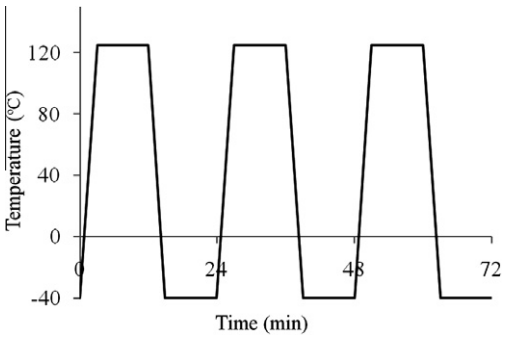

Fig. 1. A typical temperature profile with temperature range from −40 °C to 125 °C, with a 6 min ramp time and an 18 min dwell time.

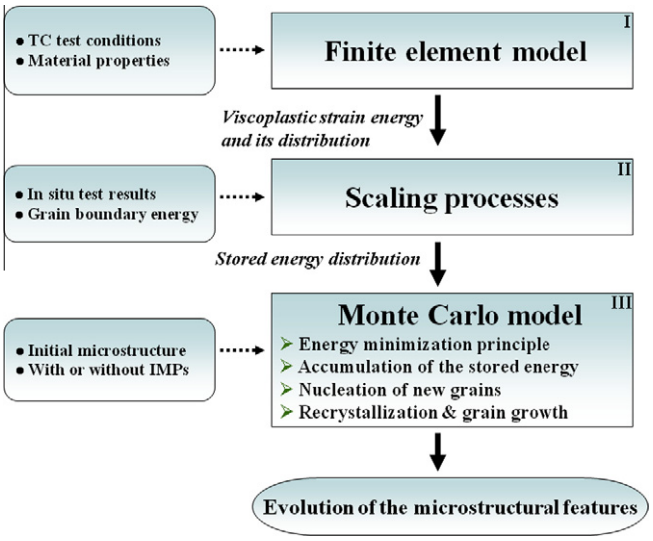

Fig. 2. Flow chart for the simulation of microstructural changes in solder interconnections.

In order to schematically describe the simulation process, a flow chart is shown in Fig. 2. There are three major steps and all the key inputs for the simulation are listed in the boxes, which are on the left side of each step. In Step I, the finite element method is employed to calculate the inelastic strain energy density of the solder interconnections under thermal cycling loads. As discussed above, it is assumed that the net increase of the stored energy takes place after every thermal cycle. In Step II (scaling processes), the stored energy, as the driving force for recrystallization, is mapped onto the lattice of the MC model, and moreover, a correlation is established to convert real time to MC simulation time with the help of the in situ test results. In Step III, the grain boundary energy and the volume stored energy are taken into consideration in the energy minimization calculations to simulate the recrystallization and grain growth processes. Furthermore, intermetallic particles (IMPs) are treated as inert particles and their influence on the distribution of stored energy is included. These three steps are discussed in detail in the following sections.

2.1. Finite element model

The 3-D finite element analysis (FEA) was performed with the help of the commercial finite element software ANSYS v.12.0. In

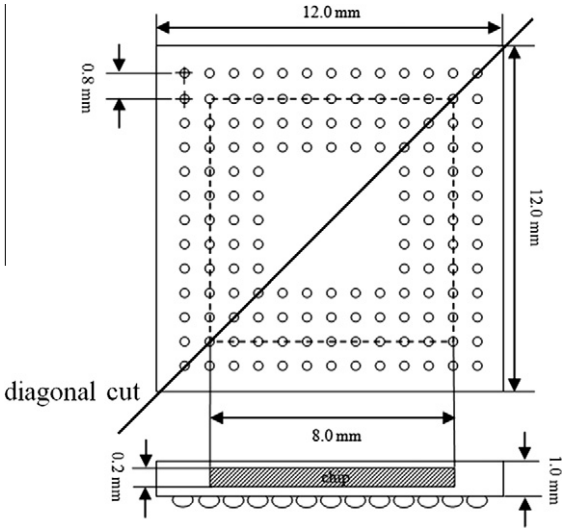

Fig. 3. Schematic show of the BGA component under study.

the experimental setup, the ball grid array (BGA) components were cut along the diagonal line before the in situ test. A schematic drawing of the BGA component is shown in Fig. 3.

Symmetrical design of the component board enabled the employment of the one-fourth model of the package during FE calculation (see Fig. 4). The symmetry boundary conditions were applied to the symmetric surfaces as mechanical constraints, and the central node of the bottom of the PWB was fixed to prevent rigid body motion. Each solder interconnection was meshed with 540 SOLID185 elements as SOLID185 has plasticity, viscoplasticity, and large strain capabilities. The rest of the model was meshed with SOLID45 elements. The total number of nodes and elements of the model was 158424 and 134379, respectively. The SnAgCu solder was modeled by Anand's constitutive model with the parameters provided by Reinikainen et al. [18]. The Anand model is often used for modeling metals behaviors under elevated temperature when the behaviors become very sensitive to strain rate, temperature, history of strain rate and temperature. The model is composed of a flow equation and three evolution equations that describes strain hardening or softening during the primary stage of creep and the secondary creep stage [19]. The inelastic strain energy is calculated by the integral of the stress with respect to the plastic strain increment.

2.2. Scaling processes

Generally speaking, there is no physically meaningful time and length scale in MC simulation, and thereby, it is difficult to compare the simulation results to experimental observations. Some calibration procedures are necessary in order to establish a relationship between real time and MC simulation time. Furthermore, the calculated inelastic strain energy needs to be converted to stored energy via a scaling process before being mapped onto the MC lattice. In the following, length scaling, time scaling and energy scaling are addressed respectively.

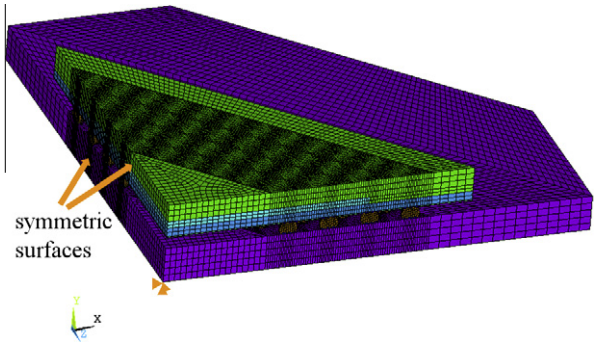

Fig. 4. Finite element model for the thermomechanical calculation.

2.2.1. Length scaling

MC simulation does not model the behavior of single atoms and accordingly is performed at the mesoscale level. An MC lattice site represents a large cluster of atoms with the typical size being in the order of micrometers. The domain of the 2-D MC simulation covers the chosen region, which belongs to the cross section of the solder interconnection. For instance, the size of the MC domain in this case is a 200×200 square lattice, which covers the $185 \times 185\ \mu m^2$ region. Thus, the unit boundary length of the MC model, s, equals 0.925 μm.

2.2.2. Time scaling

One Monte Carlo time step (MCS) is defined as N_{MC} reorientation attempts, where N_{MC} is the total number of sites in the MC lattice. This means that each site is given an opportunity to change its orientation. A correlation between the simulation time t_{MC} [MCS] and real time t [s] is usually expressed in the following form including an apparent activation energy factor (Q_m) as well as an atomic vibration frequency ($v = 8.3 \times 10^{12}$ Hz at 125 °C).

$$t_{MC} = v \exp\left(-\frac{Q_m}{RT}\right) t \tag{1}$$

where R is the universal gas constant, T is the temperature, and t is the time.

However, this time scaling process is not employed in the current study due to three main concerns. Firstly, the value of activation energy factor (Q_m) for tin is seldom reported in the literatures. Secondly, the time scaling is extremely sensitive to the value of Q_m. As shown in Table 1, a possible error of Q_m (within the range from 20 to 107 kJ/mole) leads to a significant difference in time scale, which will finally result in unreliable simulation results. Thirdly, during each thermal cycle, the temperature alternates between a low temperature and a high temperature (e.g. from −40 °C to 125 °C, see Fig. 1), which makes it difficult to use Eq. (1).

Besides the scaling approach in Eq. (1), other real time scaling approaches have also been developed and successfully applied to various applications. For instance, Safran et al. [20] set the time scale by multiplying the transition probability with a basic attempt frequency, and Raabe [21] scaled the real time step by a rate theory of grain boundary motion.

In order to improve both the accuracy and the efficiency, a new correlation between the simulation time t_{MC} [MCS] and real time t [TC] is established as follows.

$$T_{MC} = \frac{c_1}{c_2} t \tag{2}$$

where c_1 and c_2 are model parameters with the units [MCS] and [TC], respectively.

One thermal cycle is defined as the unit of time instead of using seconds. In this way, the relatively complicated temperature change within a thermal cycle is simplified and included only in

Table 1
Time scales with different activation energy factors.

Q_m (kJ/mole)	20	40	64	70	90	107
t_{MC}/t (MCS/s)	1.9e + 10	4.7e + 7	3.3e + 4	5.4e + 3	1.3e + 1	7.5e−2

the FE simulation and not in the MC simulation. The physical meaning of c_1 is the number of Monte Carlo time steps required for the growth of the newly recrystallized grains during each simulation time interval (STI). A certain amount of external energy is added to the MC lattice at the beginning of each STI and the amount of energy is calculated according to a certain number of thermal cycles, i.e. c_2. Therefore, the parameter c_2 can be considered as a time compression factor and the number of simulation time intervals is equal to t/c_2. Numerical experiments are necessary for choosing suitable values for c_1 and c_2 and the process is addressed in detail in Section 3.

2.2.3. Energy scaling

In contrast to the situation in a static recrystallization process, the stored energy of the MC sites accumulates during dynamic loading. The energy scaling procedure follows the same process as presented in our previous study [11]. First of all, the correlation between the external work and the stored energy is discussed. It is well known that a fraction of the external work, typically varying between 1% and 15%, is stored in the metallic material during deformation [22]. According to the parameter study carried out in [11] with considering the effect of recovery, the most suitable retained fraction, 5%, is used for the unrecrystallized region in the current MC simulation. Zero is assumed to be the retained fraction for the recrystallized region. This assumption is valid due to the fact that only primary recrystallization has been found in the experimental observation of solder interconnections. It should be mentioned that if non-zero retained fraction is used for the recrystallized region, the present model is capable of predicting secondary recrystallization, which may be applicable in other cases.

The energy scaling is based on the principle that the ratios of the volume stored energy to the grain boundary energy should be equated in the MC model and the physical system [23]. The driving force due to the grain boundary energy, P^{grgr}, equals $\gamma/\langle r\rangle$, where γ is the grain boundary energy per unit area and $\langle r\rangle$ is the mean grain radius. Since high angle grain boundaries are of interest to the present investigation, the value $\gamma = 0.164\ \mathrm{J/m^2}$ is used for the high angle grain boundary energy of Sn [6].

In the MC model, the driving force due to the stored energy density is given by $P^{vol}_{MC} = H/A$, where H is the volume stored energy of a site and A is the area of that site ($A = s^2$ in the 2-D square lattice). The driving force due to the grain boundary energy is given by

$$P^{grgr}_{MC} = \frac{\gamma_{MC}}{\langle r\rangle_{MC}} = \frac{J}{s\langle r\rangle_{MC}} = \frac{J}{s\langle r\rangle} \tag{3}$$

where γ_{MC} and $\langle r\rangle_{MC}$ are the grain boundary energy per unit and the mean grain radius in the MC model, respectively. Each unlike pair of nearest-neighboring sites contributes a unit of grain boundary energy J to the system. Because of the existence of the length scale factor, s, an ideal prediction should satisfy the requirement that the mean grain radiuses in the model and in the physical system are equal, $\langle r\rangle_{MC} = \langle r\rangle$.

In the physical system, the ratio of the volume stored energy to the grain boundary energy per unit volume is

$$\frac{P^{vol}}{P^{grgr}} = \frac{P^{vol}\langle r\rangle}{\gamma} \tag{4}$$

In the MC model, the ratio is given by

$$\frac{P^{vol}_{MC}}{P^{grgr}_{MC}} = \frac{H\langle r\rangle}{J s} \tag{5}$$

Equating the ratios of the model and the physical system, and rearranging, gives

$$H = \left(\frac{P^{vol} s}{\gamma}\right) J \tag{6}$$

The increment of H can be easily calculated by Eq. (6), where s and γ are known parameters. P^{vol} distribution is obtained by scaling and mapping the energy density distribution calculated by FEM onto the MC lattice. J is a unit of grain boundary energy in the MC model. It is noteworthy that the absolute value of J is not essential and knowing the ratio, H/J, is sufficient for the MC simulation.

2.3. Monte Carlo simulation of recrystallization

2.3.1. Model of nucleation

Nucleation stage is very crucial for the simulation of recrystallization. The recrystallization process is modeled by introducing nuclei (small embryos with zero stored energy) into the lattice at a constant rate, i.e. continuous nucleation. According to the locations of the valid nuclei, the nucleation is non-uniform. Although the locations of nuclei are randomly chosen, the volume stored energy of the chosen sites has to be larger than the critical stored energy, H_{cr}, before the nuclei are placed in their sites. In this way, the sites with high stored energy (e.g. near interfaces, grain boundaries, and IMPs) will have a high probability of nucleation. The critical stored energy, H_{cr}, is set to be $2J$ so that a single-site isolated embryo can grow as a new grain. Detailed discussion about the critical stored energy and critical embryo size were presented in the Ref. [23].

2.3.2. Recrystallization without the presence of IMPs

In the MC lattice, two adjacent sites with different grain orientation numbers are regarded as being separated by a grain boundary. A group of sites having the same orientation number and surrounded by grain boundaries are considered as a grain. Each site contributes an amount of stored energy, $H(S_i)$, to the system, and each pair of unlike neighboring sites contributes a unit of grain boundary energy, J, to the system. In the reorientation process, if the randomly selected site is unrecrystallized, it will be recrystallized under the condition that the total energy of the system is reduced. If the selected site is recrystallized, the reorientation process is a simulation of the nucleus growth process. The total energy of the system, E, is calculated by summing the volume stored energy and the grain boundary energy contributions throughout all the sites.

$$E = J\sum_{\langle ij\rangle}(1-\delta_{S_iS_j}) + \sum_i H(S_i) \tag{7}$$

where the sum of i is over all N_{MC} sites in the system, the sum of j is over all the nearest-neighbor sites of the site i, and δ_{ij} is the Kronecker delta. The first and second nearest neighbors are included in the energy calculation, and thereby, each site has eight nearest neighbors while square lattice is used in the current study.

2.3.3. Recrystallization with the presence of IMPs

The IMPs are introduced into the MC simulation as inert particles. They are assigned an orientation different from any of the surrounding grains and are not allowed to be reoriented during the simulation. Thus, the inert particles do not grow or move. The intermetallic particles in SnAgCu solder are mainly Cu_6Sn_5 and Ag_3Sn. The size of IMPs varies a lot and only coarse IMPs (particle size of 1 μm or above) are studied in the MC simulation. Zener-type particle pinning is not considered in the current model for the sake of simplicity. Fine particles usually prevent the motion of grain boundaries by exerting a pinning force, and therefore, suppress the progress of recrystallization. The influence of fine particles on

recrystallization has been studied in earlier work, e.g. [24]. It is believed that fine particles do not remarkably affect the distribution of stored energy within the grains; however, coarse particles exert localized stress concentrations due to the mismatch of mechanical properties and thermal expansion coefficients. Dislocation density is increased in the particle-affected deformation regions, which provide favorable sites for nucleation. To include the IMPs in the FE model as discussed in Section 2.1 is not realistic and too computationally expensive in view of the fact that the size and shape of IMPs vary a lot and the locations of IMPs are randomly distributed in the bulk solder. Instead, the size of the particle-affected deformation region is estimated and an energy amplification factor (EAF) distribution is introduced in order to consider the effects of IMPs.

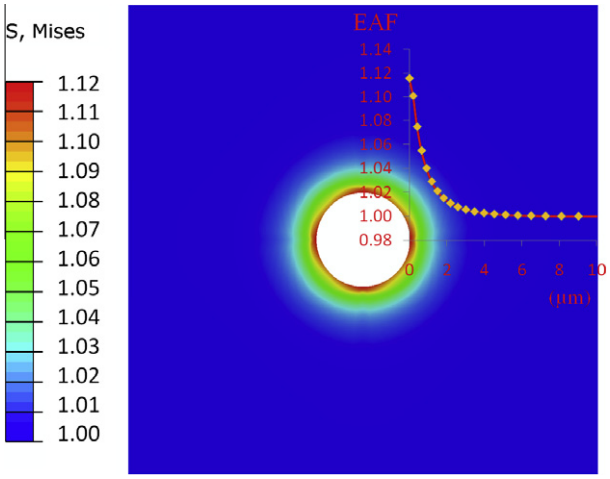

Fig. 5. von Mises stress contour and 'EAF vs. distance' curve.

A 2-D FE simulation was carried out to study the particle-affected deformation region and the energy amplification factor distribution. The model was composed of a solder matrix ($25 \times 25\ \mu m^2$) and a round IMP (radius = 5 μm). The material properties of the relatively soft solder matrix and the hard IMP were from the Ref. [25]. The loading was defined by applying the displacement on the top and right edges, i.e. bi-axial tension. The von Mises stress at the edges was not influenced by the IMP, and thereby, it was defined as one unit for the sake of normalization. The calculated stress contour and the 'EAF vs. distance' curve are shown in Fig. 5. According to the FE simulation results, the following assumptions are made with the purpose of treating IMPs in the MC simulation. Within a distance of approximately one particle radius, the calculated stored energy is amplified by a certain energy amplification factor before mapped onto the Monte Carlo lattice. The EAF for the site close to the IMP is about '1.12' and the EAF decreases linearly to '1' for the site more than one radius distance away from the IMP. In order to realize this, a new matrix storing the EAF distribution is introduced to the algorithm. Every time the stored energy of a site is updated during the recrystallization simulation, the energy increment is multiplied by the associated EAF before being added to the site. By introducing the EAF, stored energy density close to IMPs is higher than usual, leading to a higher driving force for nucleation and growth of recrystallized grains. Thus, the particle stimulated nucleation is well taken into consideration in the MC simulation.

3. Results and experimental verifications

The in situ thermal cycling tests were carried out for the verifications. During the tests, the components were taken out of the test vehicle after every 500 cycles. The solder interconnections were repolished, examined, and then put back to the test vehicle to continue the test. The microstructures of the solder cross

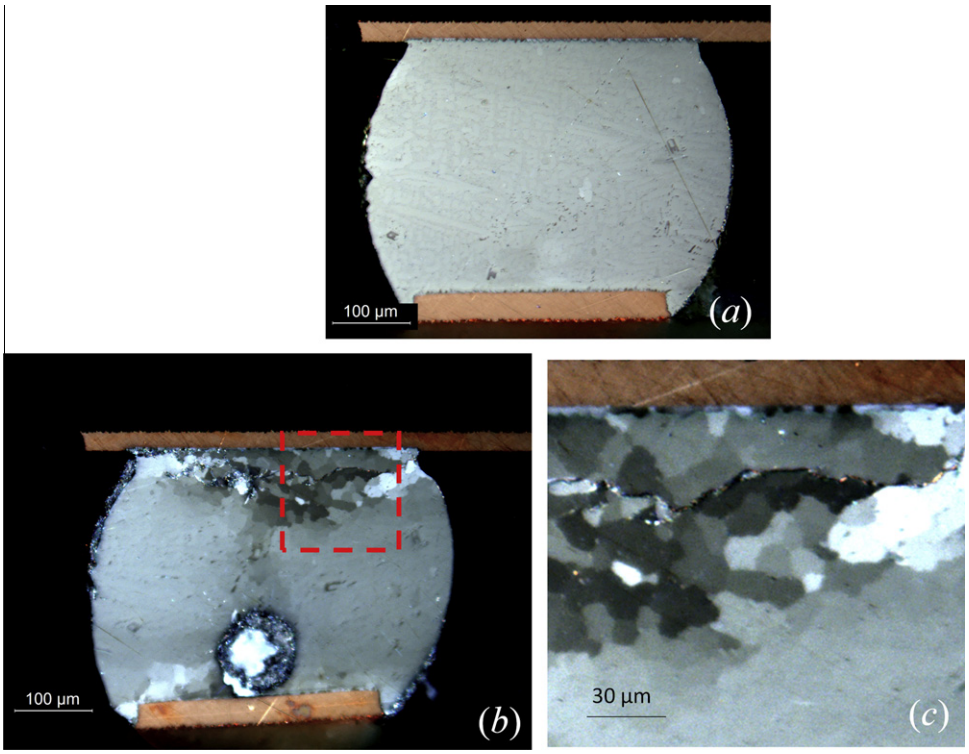

Fig. 6. Microstructure of the outermost solder interconnection observed with polarized light: (a) after solidification, (b) after 1000 thermal cycles observed with polarized light and (c) close-up view of the top right corner of the cross section.

sections were examined by optical microscopy with polarized light, which shows the areas of different orientations with different colors (see Fig. 6). The boundaries between the areas of different contrast are the high angle grain boundaries. Fig. 6a and b present the typical microstructures of an outermost solder interconnection after solidification and after 1000 in situ thermal cycling test respectively, and Fig. 6c is the close-up view of the recrystallized region. The dashed rectangle in Fig. 6b shows the domain for the microstructural simulations.

A series of numerical experiments were carried out and the simulated microstructures were compared to Fig. 6c in order to decide the suitable model parameters, c_1 and c_2, in Eq. (2) for the time scaling process. In theory, the value of the time compression factor, c_2, can range from 1 to N_{TC}, where N_{TC} is the total number of thermal cycles. In general, a larger value of c_2 leads to a more efficient calculation with less accuracy. One extreme case is when c_2 equals N_{TC}, and then, there will be only one simulation time interval and the process will be similar to a static recrystallization simulation. Considering both efficiency and accuracy, c_2 was assumed to be 100 thermal cycles, making 10 simulation time intervals for the case $N_{TC} = 1000$. Besides c_2, a number of different c_1 were studied. The microstructures of several typical values of c_1 are shown in Fig. 7. A small value of c_1, e.g. $c_1 = 10$ (see Fig. 7a) results in a small averaged grain size and immature microstructures, where newly introduced embryos do not have enough time to grow up. A large value of c_1, for instance $c_1 = 100$ (see Fig. 7d), leads to a relatively large averaged grain size as well as long and narrow grain shapes. Fig 7c is regarded as a good representative of the studied microstructure in terms of the similar averaged grain size and more or less equiaxed grain shapes. Hence, '$c_1 = 50$' was used for the rest of the simulations.

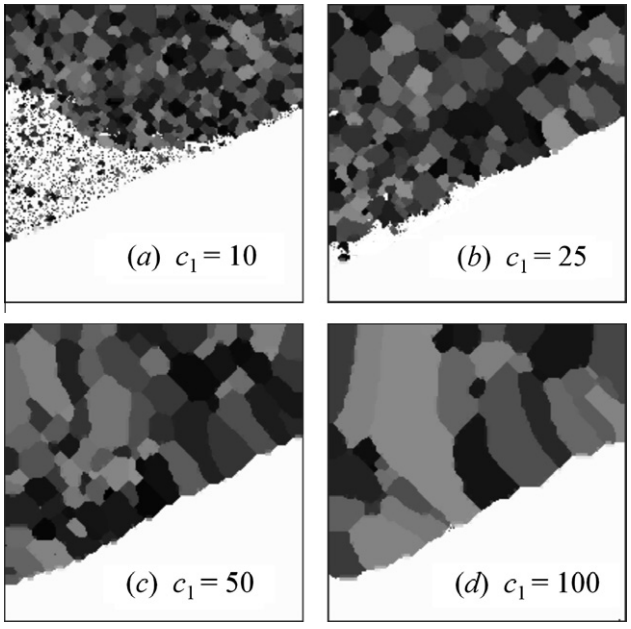

Fig. 7. Simulated microstructures with four typical c_1 values.

Another solder interconnection was selected to verify the performance of the presented algorithm. The interconnection was the second diagonal solder interconnection from the right end as shown in Fig. 4. The heterogeneous deformation of the interconnection after 1000 thermal cycles is shown in Fig. 8a. The image was taken with bright light before repolishing. The persistent slip bands are visible in the image, which show the severe plastic deformation near the interface on the component side. The distribution of the heavily deformed regions agrees well with the calculated inelastic strain energy density distribution (see Fig. 8b). This agreement verifies that the energy input for the microstructural simulation is valid. The dashed rectangle in Fig. 8b shows the domain of the following microstructural simulation.

Different from the experimental observations, the Monte Carlo simulation results offer a continuing process of the microstructural evolution. Three snapshots from the MC simulation with a time interval, 500 thermal cycles (TCs), are shown in Fig. 9. On the left side of the simulated microstructures, the related micrographs are presented. According to the simulation results, the incubation time for the recrystallization is about 400 TCs. During the incubation period, the stored energy is accumulated, but the magnitude remains below the critical value. As a result, no new grains are formed before 400 TCs. The upper right corner of the solder interconnection is the location where the highest inelastic strain energy is concentrated (see Fig. 8b). It is this very same location where the magnitude of the stored energy first exceeds the critical value and recrystallization is initiated (see Fig. 9a) and Fig. 9d). Then, as shown in Fig. 9e, the recrystallized region expands towards the lower left of the interconnection, which is in good agreement with the experimental finding (see Fig. 9b). By comparing Fig. 9e and f, it is found that the migration rate of the recrystallization front slows down during the period from 1000 TCs to 1500 TCs due to the decreasing driving force in the lattice. In the micrograph, Fig. 9c, cracks and voids are obvious, meaning that the continuity assumption of the finite

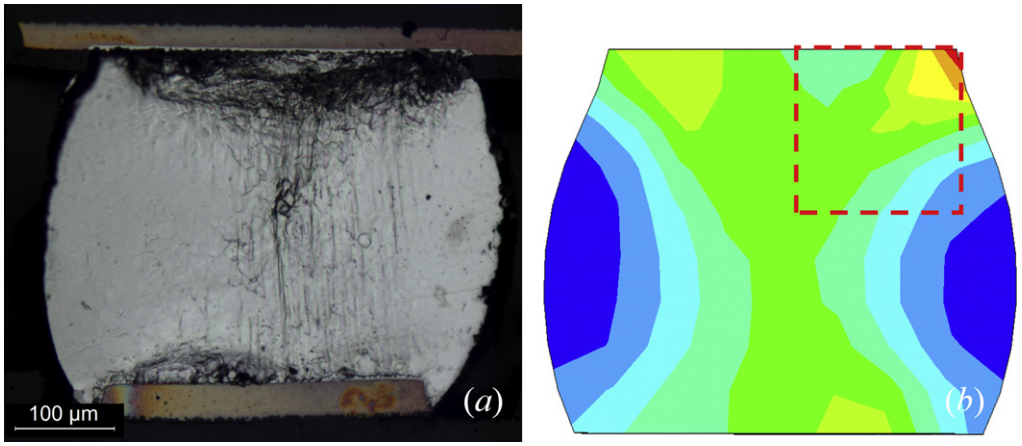

Fig. 8. (a) Plastic deformation of the solder interconnection after 1000 thermal cycles and (b) FEM-calculated inelastic strain energy density distribution, dashed rectangle shows the domain of the microstructural simulation.

element model is no longer valid. Therefore, the difference between the experimental finding and the simulated microstructure, Fig. 9f, is understandable. A possible solution is to simulate the behaviors of cracks and voids in the Monte Carlo model, output the microstructures to the finite element model, and then, use the calculated results as the inputs for the next round Monte Carlo simulation. This is to be carried out in our future work.

There was no obvious IMP-affected recrystallization in any of the in situ samples. Most of the observed recrystallized microstructures were located close to the interface region where the stored energy density was the highest. In order to focus on the influence of the IMPs and exclude the effects of the heterogeneous energy distribution, a uniform stored energy density distribution was assumed during the simulation. The assumption is valid when the calculation domain is located in the center part of the solder interconnection, where the energy magnitude is relatively low and energy distribution is quite uniform. Furthermore, the energy amplification factors introduced in Section 2.3.3 were used to increase the energy around the IMPs.

A micrograph from a normal thermal cycling test was used to verify the simulation results (see Fig. 10a). The sample was examined after 5000 TCs and the micrograph was taken from the center of the cross section. The major IMPs were highlighted in Fig. 10a for easy recognition and Fig. 10b was used as the initial microstructure for the microstructural simulation. As compared with in situ samples, solder interconnections in normal thermal cycling tests experience moderate plastic deformation, and thereby, require long incubation time for recrystallization.

Four snapshots (after 1500, 3000, 4000, and 5000 TCs respectively) of the simulated microstructural evolution are presented in Fig. 11. Since there are no interfaces and pre-existing grain

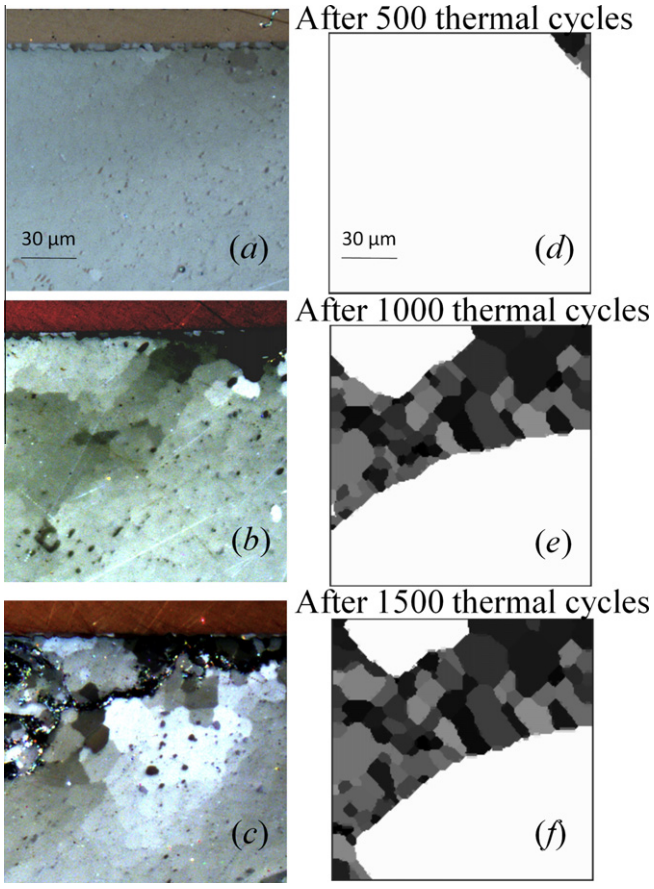

Fig. 9. (a), (b), and (c) are experimentally observed microstructures of the same location; (d), (e), and (f) are simulated microstructures after 500, 1000, and 1500 thermal cycles respectively.

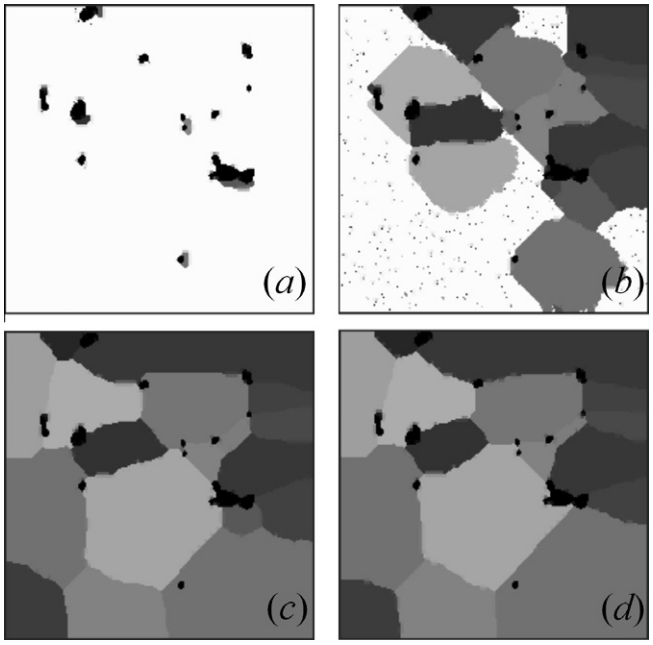

Fig. 11. Simulated microstructural evolution with the present of IMPs: (a) after 1500 TCs, (b) after 3000 TCs, (c) after 4000 TCs and (d) after 5000 TCs.

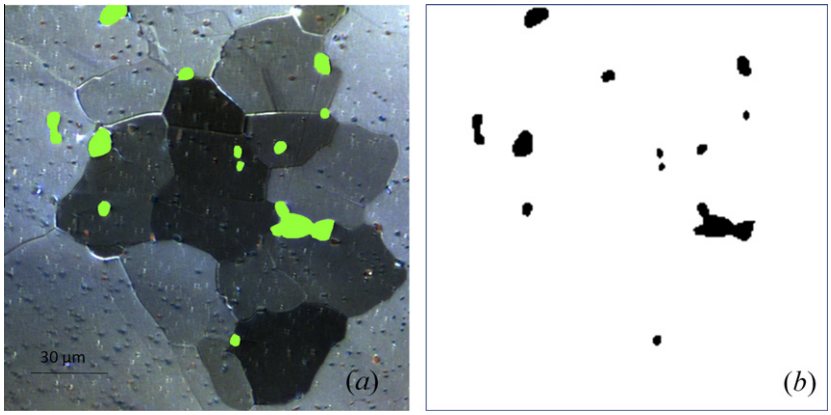

Fig. 10. (a) Micrograph shows IMP-affected recrystallization, (b) initial microstructure for the Monte Carlo simulation.

boundaries in the calculation domain, the intermetallic particles are the most favorable sites for nucleation in this case. The particle stimulated nucleation is shown in the simulation results and the initiation of recrystallization near the IMPs is clearly visible in Fig. 11a. The growth of the new grains at the expense of the strain-hardened matrix is presented in Fig. 11b–d. After 4000 TCs, since the whole matrix is consumed by the recrystallized grains and most of the stored energy is released, there is practically no difference between Fig. 11c and d. Furthermore, it is found that the IMPs tend to located at the grain boundaries or triple junctions of the new grains as a result of the energy minimization calculation, which is consistent with the experimental results (see Fig. 10a).

4. Conclusions

In this work, a new algorithm was developed in order to predict dynamic recrystallization in solder interconnections during thermal cycling tests. The approach was realized by combining a Potts model based Monte Carlo method and a finite element method. The correlation between real time and MC simulation time was established with the help of the in situ test results. Recrystallization with the presence of intermetallic particles in solder matrix was for the first time simulated by introducing the energy amplification factors in the particle-affected deformation regions.

The algorithm predicts the incubation period of the recrystallization as well as the growth tendency of the recrystallized region, which are in good agreement with the experimental findings. With appropriate modifications, the algorithm can be applied to solder interconnections subjected to power cycling tests and even for field conditions. Although the research for the microstructural simulation of solder interconnections is still at its primary stage, the presented algorithm shows potential for better reliability assessment of solder interconnections used in the electronics industry.

Acknowledgements

The authors would like to thank the Finnish Funding Agency for Technology and Innovation (TEKES), Nokia, Efore Plc, NXP Semiconductors, Salon Teknopaja Oy and National Semiconductor for supporting the research. The Finnish IT Center for Science (CSC) is also gratefully acknowledged for providing computer facilities and software.

References

[1] T.T. Mattila, V. Vuorinen, J.K. Kivilahti, J. Mater. Res. 19 (2004) 3214–3223.
[2] D. Henderson, J.J. Woods, T.A. Gosseling, J. Bartelo, D.E. King, T.M. Korhonen, M.A. Korhonen, L.P. Lehman, E.J. Cotts, S.K. Kang, P. Lauro, D.-Y. Shih, C. Goldsmith, K.J. Puttliz, J. Mater. Res. 19 (2004) 1608–1612.
[3] S. Terashima, K. Takahama, M. Nozaki, M. Tanaka, T. Mater, JIM 45 (2004) 1383–1390.
[4] S. Dunford, S. Canumalla, P. Viswanadham, in: Proc. 54th ECTC, 2004, pp. 726–736.
[5] J.J. Sundelin, S.T. Nurmi, T.K. Lepistö, Mater. Sci. Eng. A 474 (2008) 201–207.
[6] F.J. Humphreys, M. Hatherly, Recrystallization and Related Annealing Phenomena, second ed., Elsevier Science, Oxford, 2004.
[7] R.D. Doherty, D.A. Hughes, F.J. Humphreys, J.J. Jonas, D.J. Jensen, M.E. Kassner, W.E. King, T.R. McNelley, H.J. McQueen, A.D. Rollet, Mater. Sci. Eng. A 238 (1997) 219–274.
[8] K. Nurminen, Master's thesis (in Finnish), TKK, Espoo, Finland, 2006.
[9] M.A. Miodownik, J. Light Met. 2 (2002) 125–135.
[10] N. Yazdipour, C.H.J. Davies, P.D. Hodgson, Comput. Mater. Sci. 44 (2008) 566–576.
[11] J. Li, T.T. Mattila, J.K. Kivilahti, J. Electron. Mater. 39 (2010) 77–84.
[12] A.D. Rollett, D. Raabe, Comput. Mater. Sci. 21 (2001) 69–78.
[13] X. Song, M. Rettenmayr, Mater. Sci. Eng. A 332 (2002) 153–160.
[14] Q. Yu, S.K. Esche, J. Mater. Process. Technol. 169 (2005) 493–502.
[15] C. Zambaldi, F. Roters, D. Raabe, U. Glatzel, Mater. Sci. Eng. A. 454–455 (2007) 433–440.
[16] D. Raabe, R.C. Becker, Modelling Simul. Mater. Sci. Eng. 8 (2000) 445–462.
[17] JESD22-A104C, 2005. Temperature cycling, Arlington, Virginia: JEDEC Solid State Technology Association. <http://jedec.org/download/search/22a104c.pdf>.
[18] T. O. Reinikainen, P. Marjamäki, J. K. Kivilahti, in: Proc. 6th EuroSim Conf., 2005, pp. 91–98.
[19] L. Anand, J. Eng Mater. Technol. ASME 104 (1982) 12–17.
[20] B.A. Safran, P.S. Sahni, G.S. Grest, Phys. Rev. B 28 (1983) 2693–2704.
[21] D. Raabe, Acta Mater. 48 (2000) 1617–1628.
[22] M.B. Bever, D.L. Holt, A.L. Tichener, Prog. Mat. Sci. 17 (1973) 1–190.
[23] A.D. Rollett, P. Manohar, Continuum Scale Simulation of Engineering Materials: Fundamentals-Microstructures-Process Applications, in: D. Raabe et al. (Eds.), Wiley-VCH, Weinheim, 2004 (Chapter 4).
[24] D. Raabe, L. Hantcherli, Comput. Mater. Sci. 34 (2005) 299–313.
[25] R.R. Chromik, R.P. Vinci, S.L. Allen, M.R. Notis, J. Min. Met. Mat. s. June (2003) 66–69.